

Experimental determination of solubilities of magnesium borates: Solubility constants of boracite $[\text{Mg}_3\text{B}_7\text{O}_{13}\text{Cl}(\text{cr})]$ and aksaite $[\text{MgB}_6\text{O}_7(\text{OH})_6 \cdot 2\text{H}_2\text{O}(\text{cr})]$

Yongliang Xiong*, Leslie Kirkes, Jandi Knox, Cassie Marrs, Heather Burton

Sandia National Laboratories (SNL), Carlsbad Programs Group, 4100 National Parks Highway, Carlsbad, NM 88220, USA

ARTICLE INFO

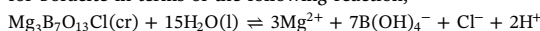
Editor: K Johannesson

Keywords:

Borate deposits
Salt formations
Salt lakes
Borax
Sodium tetraborate
Pitzer model

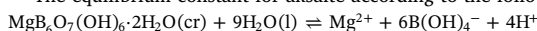
ABSTRACT

In this study, solubility measurements regarding boracite $[\text{Mg}_3\text{B}_7\text{O}_{13}\text{Cl}(\text{cr})]$ and aksaite $[\text{MgB}_6\text{O}_7(\text{OH})_6 \cdot 2\text{H}_2\text{O}(\text{cr})]$ from the direction of supersaturation were conducted at $22.5 \pm 0.5^\circ\text{C}$. The equilibrium constant ($\log_{10}K^0$) for boracite in terms of the following reaction,



is determined as -29.49 ± 0.39 (2σ) in this study.

The equilibrium constant for aksaite according to the following reaction,



is determined as -44.41 ± 0.41 (2σ) in this work.

This work recommends a set of thermodynamic properties for aksaite at 25°C and 1 bar as follows: $\Delta H_f^0 = -6063.70 \pm 4.85 \text{ kJ}\cdot\text{mol}^{-1}$, $\Delta G_f^0 = -5492.55 \pm 2.32 \text{ kJ}\cdot\text{mol}^{-1}$, and $S^0 = 344.62 \pm 1.85 \text{ J}\cdot\text{mol}^{-1}\cdot\text{K}^{-1}$. Among them, ΔG_f^0 is derived from the equilibrium constant for aksaite determined by this study; ΔH_f^0 is from the literature, determined by calorimetry; and S^0 is computed in the present work from ΔG_f^0 and ΔH_f^0 .

This investigation also recommends a set of thermodynamic properties for boracite at 25°C and 1 bar as follows: $\Delta H_f^0 = -6575.02 \pm 2.25 \text{ kJ}\cdot\text{mol}^{-1}$, $\Delta G_f^0 = -6178.35 \pm 2.25 \text{ kJ}\cdot\text{mol}^{-1}$, and $S^0 = 253.6 \pm 0.5 \text{ J}\cdot\text{mol}^{-1}\cdot\text{K}^{-1}$. Among them, ΔG_f^0 is derived from the equilibrium constant for boracite determined by this study; S^0 is from the literature, determined by calorimetry; and ΔH_f^0 is computed in this work from ΔG_f^0 and S^0 .

The thermodynamic properties determined in this study can find applications in many fields. For instance, in the field of material science, boracite has many useful properties including ferroelectric and ferroelastic properties. The equilibrium constant of boracite determined in this work will provide guidance for economic synthesis of boracite in an aqueous medium. Similarly, in the field of nuclear waste management, iodide boracite $[\text{Mg}_3\text{B}_7\text{O}_{13}\text{I}(\text{cr})]$ is proposed as a waste form for radioactive ^{129}I . Therefore, the solubility constant for chloride boracite $[\text{Mg}_3\text{B}_7\text{O}_{13}\text{Cl}(\text{cr})]$ will provide the guidance for the performance of iodide boracite in geological repositories. Boracite/aksaite themselves in geological repositories in salt formations may be solubility-controlling phase(s) for borate. Consequently, solubility constants of boracite and aksaite will enable researchers to predict borate concentrations in equilibrium with boracite/aksaite in salt formations.

1. Introduction

Boracites with a general formula $\text{M}_3\text{B}_7\text{O}_{13}\text{X}$ ($\text{M} = \text{Mg}$, and transition elements Cr, Mn, Fe, Co, Ni, Cu, Zn, or Cd; $\text{X} = \text{halide}$, F, Cl, Br, or I) constitute a large group of isomorphous compounds with > 20 species (Li et al., 2003). Among them, the boracite end member with Mg

and Cl, i.e., $\text{Mg}_3\text{B}_7\text{O}_{13}\text{Cl}$, is an important borate mineral, especially for material science (e.g., Ostrovsky and Berger, 2017). In the following, unless otherwise noted, boracite refers to the end member with Mg and Cl for simplicity. It occurs in evaporate deposits in salt formations (e.g., Phillips, 1947; Braitsch, 1971; Green and Freier, 2010; Gao et al., 2012; Zhang et al., 2013), and the description about its occurrence appeared

* Corresponding author.

E-mail address: yxiong@sandia.gov (Y. Xiong).

<https://doi.org/10.1016/j.chemgeo.2018.02.008>

Received 26 October 2017; Received in revised form 28 January 2018; Accepted 2 February 2018
0009-2541/ © 2018 Elsevier B.V. All rights reserved.

in the literature as early as in the nineteenth century (Magtear, 1869; Cadell, 1885), and it is also present in salt lakes (e.g., Heggemann et al., 1994; Zheng, 1997). Boracite appears in salt formations in various assemblages. In the salt formation in the Khorat basin in Thailand, boracite co-exists with carnallite ($\text{KMgCl}_3 \cdot 6\text{H}_2\text{O}$) and bischofite ($\text{MgCl}_2 \cdot 6\text{H}_2\text{O}$) (Le, 1986). In the field of material science, boracites have many useful properties including ferroelectric and ferroelastic properties (e.g., Torre et al., 1972).

Aksaite with a structural formula of $\text{MgB}_6\text{O}_7(\text{OH})_6 \cdot 2\text{H}_2\text{O}(\text{cr})$ is a magnesium borate mineral, which was discovered in 1960's (Clark and Erd, 1963; Dal Negro et al., 1971). It is also present in evaporate deposits in salt formations (Valeyev et al., 1973; Garrett, 1998), and in salt lakes (Li et al., 2012).

In the field of nuclear waste management, as boracite and aksaite are present in evaporate deposits in salt formations mentioned before, they are potentially important to geological repositories in salt formations. Salt formations are considered to be ideal for nuclear waste isolation (National Academy of Science, 1957). Recent investigations have suggested that borate could potentially complex with Nd(III) (Borkowski et al., 2010; Xiong, 2017), an analog to Am(III) in chemical behavior. Hence, a comprehensive understanding of interactions of borate with major ions in brines as well as the potential solubility-controlling phase(s) for borate is needed to accurately describe the contributions of borate to the potential solubility of Am(III) in brines in salt formations, as they contain significant concentrations of borate.

In brines associated with salt formations, they contain high concentrations of chloride along with significant concentrations of boron and magnesium. For instance, at the Waste Isolation Pilot Plant (WIPP), a U.S. Department of Energy geological repository for the permanent disposal of defense-related transuranic (TRU) waste (U.S. DOE, 1996), the Generic Weep Brine (GWB) and Energy Research and Development Administration Well 6 (ERDA-6), contain high concentrations of chloride (i.e., 6.40 and 5.27 $\text{mol} \cdot \text{kg}^{-1}$ for GWB and ERDA-6, respectively), borate (i.e., 0.180 and 0.0692 $\text{mol} \cdot \text{kg}^{-1}$ for GWB and ERDA-6, respectively) and magnesium (i.e., 1.16 and 0.0209 $\text{mol} \cdot \text{kg}^{-1}$ for GWB and ERDA-6, respectively) (Xiong and Lord, 2008). Consequently, in geological repositories in salt formations, the interactions among chloride, borate, and magnesium, will be important to the accurate description of the contributions of borate to the solubility of Am(III) in brines in salt formations.

In addition, iodide-boracites, ($\text{M}_3\text{B}_7\text{O}_{13}\text{I}$, where M represents various divalent metal ions), have been proposed as a waste form for radioactive iodine, ^{129}I , in the field of nuclear waste management (e.g., Vance et al., 1981).

Thermodynamic properties of boracite are not well known. Anovitz and Hemingway (2002) listed the Gibbs free energy of formation for boracite from an unpublished source from Khodakovskiy, Semenov and Aksaenova (see Pages 196, 252 in Anovitz and Hemingway, 2002). Regarding aksaite, Jia et al. (1999) determined its enthalpy of formation using the calorimetric method. However, its Gibbs free energy of formation has not been determined, and therefore its solubility constant is unknown. The knowledge of the sets of thermodynamic properties for aksaite and boracite will be useful to many fields. For this reason, we determine the solubility constants of boracite and aksaite in this work. Then, based on our solubility constants, we are able to provide the sets of thermodynamic properties for aksaite and boracite. The recommended sets of thermodynamic properties for boracite and aksaite may find applications in many fields. For instance, aksaite double salt has been observed in Da Chaidam Salt Lake and Xiao Chaidam Salt Lake (Li et al., 2012). Therefore, the thermodynamic properties of aksaite can be used to elucidate the conditions for the formation of aksaite in those salt lakes, including temperature variations.

2. Experimental methods

In our solubility experiments, we performed the solubility measurements from the direction of supersaturation. All chemicals used in our experiment were ACS reagent grade.

In our supersaturation experiment, we first placed 250 mL of a 1.0 $\text{mol} \cdot \text{kg}^{-1}$ MgCl_2 solution into a glass beaker with a stir bar. Then, 8.5023 g of H_3BO_3 was added into the above solution. The solution was well mixed until all of H_3BO_3 was dissolved. After that, 2.0114 $\text{mol} \cdot \text{dm}^{-3}$ NaOH was dropwise added into the above solution to initiate precipitation. Finally, the solution with precipitates was transferred from the glass beaker into a 500 mL plastic bottle for storage of the supersaturation experiment at $22.5 \pm 0.5^\circ\text{C}$. The experiment was sampled after 970 days.

The pH readings were measured with an Orion-Ross combination pH glass electrode, coupled with an Orion Research EA 940 pH meter that was calibrated with three pH buffers (pH 4, pH 7, and pH 10). Negative logarithms of hydrogen-ion concentrations on molar scale (pCH) were determined from pH readings by using correction factors (Hansen, 2001). Based on the equation in Xiong et al. (2010), pCHs are converted to negative logarithms of hydrogen-ion concentrations on molal scale, pH_m , a notation from Oak Ridge National Laboratory/University of Idaho (e.g., Wood et al., 2002).

Solution samples were periodically withdrawn from experimental runs. Before solution samples were taken, pH readings of experimental runs were first measured. The sample size was usually 3 mL. After a solution sample was withdrawn from an experiment and filtered with a 0.2 μm syringe filter, the filtered solution was then weighed, acidified with 0.5 mL of concentrated TraceMetal® grade HNO_3 from Fisher Scientific, and finally diluted to a volume of 10 mL with DI water. If subsequent dilutions were needed, aliquots were taken from the first dilution samples for the second dilution, and aliquots of the second dilution were then taken for the further dilution.

Boron, sodium and magnesium concentrations of solutions were analyzed with a Perkin Elmer dual-view inductively coupled plasma-atomic emission spectrometer (ICP-AES) (Perkin Elmer DV 8300). Calibration blanks and standards were precisely matched with experimental matrices. The linear correlation coefficients of calibration curves in all measurements were better than 0.9995. The analytical precision for ICP-AES is better than 1.00% in terms of the relative standard deviation (RSD) based on replicate analyses.

Chloride concentrations were analyzed with a DIONEX ion chromatograph (IC) (DIONEX IC 3000).

The solid phase identification was performed by using a Bruker AXS, Inc., D8 Advance X-ray diffractometer (XRD) with a Sol-X detector. XRD patterns were collected using $\text{CuK}\alpha$ radiation at a scanning rate of $1.33^\circ/\text{min}$ for a 2θ range of $10\text{--}90^\circ$.

3. Experimental results

Fig. 1 shows the XRD patterns for our supersaturation experiment with an initial concentration of 1.0 $\text{mol} \cdot \text{kg}^{-1}$ MgCl_2 solution. Fig. 1 shows that boracite along with aksaite crystallized from the solution. Notice that the peaks characteristic of boracite and aksaite, are present in the XRD patterns for our experiment (Fig. 1).

Experimental results are tabulated in Table 1. In Fig. 2, total boron, chloride, magnesium and sodium concentrations as a function of experimental time are displayed, respectively. From Fig. 2, we can see that the equilibrium was established at the experimental duration ≥ 970 days. The duration of our experiment was long, and it was up to 1642 days (Table 1, Fig. 2).

Download English Version:

<https://daneshyari.com/en/article/8910285>

Download Persian Version:

<https://daneshyari.com/article/8910285>

[Daneshyari.com](https://daneshyari.com)